A Comparison of Methods for Estimating Q

Xiong Lei and Eugene C. Morgan, Pennsylvania State University*

Summary

Quality factor (Q) as a quantitative measurement of seismic absorption can be used as a hydrocarbon indicator, to implement deconvolution, or in forward modeling. However, quality factor remains difficult to reliably measure from seismic data. A lot of approaches in either the time or frequency domain have been proposed in the past. A good performance was validated in either VSP, crosswell, or sonic waveform data. However, accurate Q extraction needs amplitude or spectrum preservation processing. So, it is, especially for pre-stack data, still challenging because of much more noise interference and more difficult interface tracking. Detailed analysis and comparison of those methods, especially for commonly used centroid frequency shift method, spectral ratio method and peak frequency method, are necessary when estimating Q from reflection data. Beside, in this paper some data pre-processing techniques which aim to improve the accuracy of Q estimation were discussed.

Introduction

In seismic survey interpretation, quality factor (Q) is an important geologic attribute. It is associated with the intrinsic physical properties of rocks and fluids (Winkler & Nur, 1982; Sheriff and Geldart, 1995), as well as scattering effects of the seismic wave (Goutbeek, et al., 2004). Since the intrinsic Q is more related to the physical properties of rocks and fluids, it can better serve as a valuable diagnostic tool for reservoir characterization and hydrocarbon detection (Toksöz, et al., 1979; Frisillo and Stewart, 1980). Additionally, the intrinsic Q is crucial to interpret the effects of AVO, improve the resolution of seismic imaging, and advance the study of material properties. However, intrinsic Q remains a difficult seismic attribute to measure from field data, and few guidelines exist that speak to the reliability of methods for estimating Q.

Currently, many methods exist to estimate quality factor from seismic transmission data, such as VSP (e.g., Hauge 1985) and crosswell (e.g. Quan and Harris 1997; Neep et al. 1996); or seismic reflection data, such as single stacked common-depth-point (CDP) reflection data (e.g., Jannsen, et al, 1985; Tonn, 1991) and common midpoint (CMP) gather data (e.g., Dasgupta and Clark, 1998; Hackert and Parra, 2004). These methods operate in either the time domain or frequency domain. For time domain methods, the simplest one is the amplitude decay method, e.g., the risetime approach (Gladwin and Stacey, 1974). Others approaches include wavelet modeling (Jannsen et al., 1985), analytical signal method (Engelhard, 1996), and matching filter method (Cheng and Margrave, 2013).

However, due to the mingling of scattering attenuation with intrinsic attenuation, all time-domain methods above cannot be as accurate as spectrum ones, since the frequency is not affected by scattering. For example, the spectral ratio method (Bath, 1974; Hauge, 1981) obtains relatively accurate quality factor measurements from the logarithm ratio of amplitude spectra and assumes that spherical spreading and scattering is frequency-independent. While this method is commonly adopted in practice, previous studies (e.g., Tu and Lu, 2010) note that the estimated quality factor is sensitive to spectral notching and choice of bandwidth. Instead of using spectral ratio, Quan and Harris (1997) presented a centroid frequency shift method to estimate quality factor in an inhomogeneous medium. Like other spectral approaches, it has a strong capability to resist interference from frequency-independent noise. The methods above are all for post-stack or single trace data. For surface common-midpoint (CMP) gather data, Dasgupta and Clark (1998) proposed a quality factor-versus-offset (QVO) method. Hackert and Parra (2004) improved the QVO to remove tuning effects by using well-log based localized spectral correction. The latest method for surface CMP gather data is the peak frequency shift method (Zhang and Ulrych, 2002). They calculated quality factor from peak frequency variations of a reflection at different offsets. This method can be applied to both CMP gathers and post-stack data. Another notable spectral method is the spectrum modeling method (Jannsen et al., 1985; Tonn, 1991), which is a by-product of the wavelet modeling method (Jannsen et al., 1985; Tonn, 1991) and a frequency-domain alternative to the matching filter method (Cheng and Margrave, 2013).

In this paper, we compare popular methods for measuring intrinsic Q, and focus on the frequency domain methods: spectral ratio method (SRM), centroid frequency shift method (CFS), and peak frequency shift method (PFS). These relatively popular methods have shown greater success in the literature than other methods.

Quality Factor Measurement

(1) Spectral Ratio Method (SRM): For the purpose of estimating attenuation, the process of wave propagation is described by a linear system theory. If the spectrum of seismic source wavelet is $S(f)$, the absorption response is $H(f)$, geometrical spreading and transmission response are included in $G(f)$, and the received amplitude spectrum is $R(f)$. Then we have the following expression

$$\ln\left(\frac{R(f)}{S(f)}\right) = -\frac{\pi t}{Q} f + \ln G \qquad (1)$$

So, Q can be found from the slope of a line fitted to the log ratio of the two spectra versus frequency.

(2) Centroid Frequency Shift Method (CFS): As proposed in Quan and Harris (1997), if the incident spectrum is Gaussian, the quality factor is as follows,

$$Q = \frac{\pi(t_r - t_s)\sigma_s^2}{f_s - f_r} \qquad (2)$$

Where the centroid frequencies f_s, f_r and spectral variance σ^2 are defined by

$$f_c = \frac{\int f \cdot |S(f)| df}{\int |S(f)| df}, \sigma_s^2 = \frac{\int (f - f_s)^2 \cdot |S(f)| df}{\int |S(f)| df} \qquad (3)$$

(3) Peak Frequency Shift Method (PFS): The Q is expressed as a function of the peak frequency f_p and the dominant frequency f_m.

$$Q = \frac{\pi t f_p f_m^2}{2(f_m^2 - f_p^2)} \quad (4)$$

Where f_p is the frequency of maximum amplitude in the specrum. f_m can be estimated by the following equation once we know the peak frequency f_{p1} at time t_1 and f_{p2} at time t_2.

$$f_m = \sqrt{\frac{f_{p1} f_{p2} (t_2 f_{p1} - t_1 f_{p2})}{t_2 f_{p2} - t_1 f_{p1}}} \quad (5)$$

However, any given method cannot be expected to work perfectly under all conditions (Tonn, 1991). Here, the purpose of our work is to investigate the performance of these three popular methods stated above. However, the success of any given method is dependent on any pre-processing done to the amplitude data. The next section of this paper discusses the five different data pre-processing techniques we consider. Following this, we evaluate the performance of the various combinations of techniques and methods using synthetic seismic reflection data. The goal of this study is to comprehensively diagnose these methods under condition of different pre-processing techniques, and to ultimately provide insight on the optimal combination of pre-processing techniques and Q estimation methods.

Methodology

The different kinds of noise caused by the ambient condition, equipment, or personal error would distort the time or frequency characteristics of the signal, affecting the accuracy of Q estimation. Such noise leads to the demand for data pre-processing procedures before quality factor measurement. However, excessive processing would cut down the reliability of estimation. The degree of pre-processing, such as how much bandpass filter we would use, what kind of window function to impose, what kind of time-frequency decomposition techniques to apply, deserves further researching.

In particular, the quality of the estimates from the frequency-based methods above largely depends on the quality of the time-frequency decomposition being used. The traditional Fast Fourier Transform (FFT) suffers from trade-off in time localization and spectral resolution, where smaller window size will be more representative of the target interface, but the resulting spectrum will be more poorly resolved. Using a continuous wavelet transform (CWT) instead of FFT affords better time resolution without the subjectivity of window choice. However, this comes at the cost of subjectivity in the choice of mother wavelet to use a basis in the transform. One would want this mother wavelet to resemble the source wavelet, but in practice the source wavelet may be unknown. In this section, we describe the five different candidate pre-processing workflows that focus on exploring the impact of CWT over FFT.

Technique I: At first, we implement a bandpass filter with lower and upper cutoffs of 10 and 150 Hz to eliminate random noise for data with 60Hz dominant frequency. Secondly, we utilize a Hamming window to select the data surrounding the target interfaces in case of frequency leakage when using FFT to do spectral transformation. This keeps the high frequency resolution and is easily implemented (Harris, 1978). Then, the time series from each window are transformed to the frequency domain via FFT after zero-padding to improve the spectral resolution. Sometimes, leftover noise in the signals can propagate into the spectra. A moving average filter is then used to smooth the curves of the spectra (Karl, 1989). Either of the three methods above then use these smoothed spectra. These steps are displayed conceptually in Fig. 1.

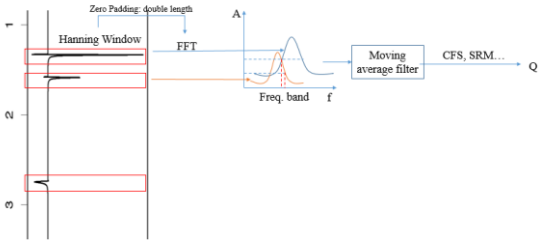

Fig. 1 Schematic diagram of technique I

Technique II: Initially, the same bandpass filter and subsequent Hamming window as in Technique I are implemented on the signal. Next we apply the CWT with a Morlet mother wavelet to the target reflection data obtaining its time-frequency scalogram (Fig. 2). Then the time slice of the scalogram for a given interface at maximum amplitude is picked up as the input amplitude spectrum. Again, moving average filtering is performed prior to Q estimation.

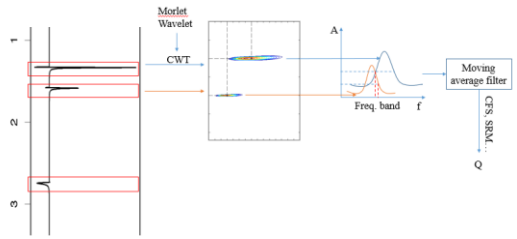

Fig. 2 Schematic diagram of technique II

Technique III: Here, all the steps are the same as in Technique II, except the assumed Morlet wavelet is replaced by a statistically extracted wavelet. We use the wavelet extraction technique of Lu et al. (2007) on the target windowed data. Then, the estimated wavelet is used as the mother wavelet for CWT. Compare Fig. 2 and 3 for the operational differences between Techniques II and III, respectively.

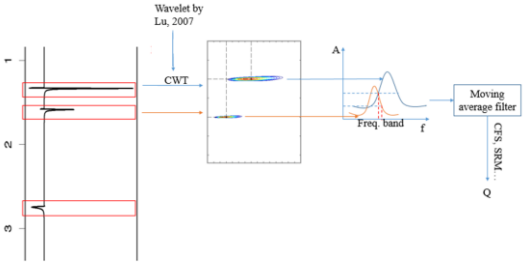

Fig. 3 Schematic diagram of technique III

Technique IV: After denoising, here we use FFT to transform the estimated wavelet by Lu's method into the

frequency domain. Before doing FFT, the Hamming window and zero padding technique are also implemented on the wavelet (Fig. 4). Then the moving average filter smooths the spectra before Q estimation.

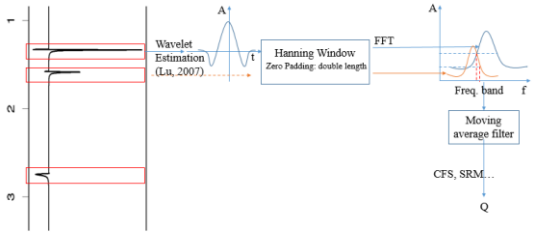

Fig. 4 Schematic diagram of technique IV

Technique V: As illustrated in Fig. 5, the last approach is to implement the CWT with a Morlet mother wavelet on the estimated wavelet by Lu's method. This differs from Technique III in that here the CWT is being performed on the extracted wavelet, whereas in III the extracted wavelet is being used as the basis for the CWT being run on the signal.

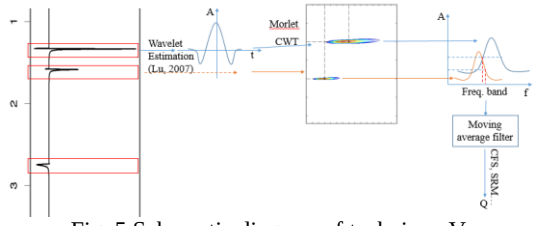

Fig. 5 Schematic diagram of technique V

Lastly, an important factor that determines the accuracy of Q estimation is the choice of an effective bandwidth, which is applied to each spectrum after the pre-processing technique and before the Q estimation method. Tu and Lu (2010) suggest determining the effective bandwidth by the peak frequency and an effective-bandwidth coefficient ε.

$$f_{eff} \in \{S(f) \geq \varepsilon \cdot \max(|S(f)|)\} \quad (6)$$

In addition to the five techniques and three methods described above, we also included ten coefficients in our study: ε = (0, 0.1, …, 0.9).

Numerical Example

In this part, a 1D synthetic model was created to test the validation of those methods. The quality factor of the geological model varied over the following values: 10, 20, 50, 80, 120, and 200 (one example as figure 6). The simulating wavelet is generated from the Berlage model (Aldridge, 1990),

$$b_0 = H(t)t^n \exp(-\alpha t)\cos(2\pi f_p t + \phi_0) \quad (7)$$

Where the dominant frequency f_p is 60Hz, the sampling interval time is 0.002s. $H(t)=1$ when $t>0$, $H(t)=0$ when $t \leqslant 0$. $a=200$, $\phi_0 = -0.5\pi$ and $t \in [-0.052, 0.076]$. The target wavelet is calculated based on the scattering and absorption theorem. For each Q value above, 100 synthetic traces are generated with separation time between reflections varying according to a normal distribution with mean of 400ms (Figure 7). Here we specifically do not include noise or tuning effects so that we can achieve a baseline evaluation of the methods and techniques under ideal conditions. These factors will be investigated in future work.

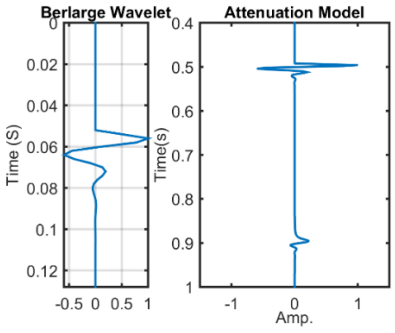

Fig. 6 Attenuation model: Q = 20

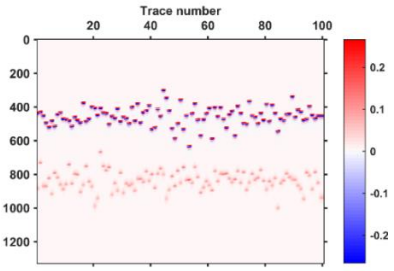

Fig. 7 100 Normal distributed traces (Q=20)

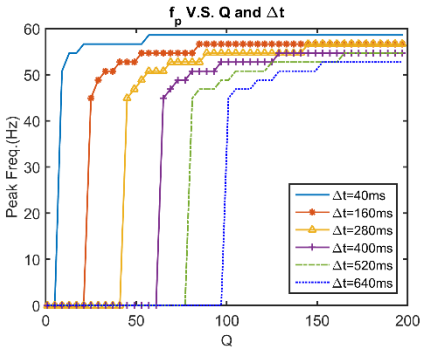

Fig. 8 Peak frequency versus Q for different separation times (corresponding to layer thickness). The original source wavelet is 60Hz Berlage wavelet. For instance, for layer of Q<60, after travelling 400ms, the peak frequency of the wavelet is equal to zero. It fails to implement PFS.

Results and Discussion

Firstly, we note a limitation of the PFS method (using all techniques), in that it does not achieve reliable estimates under high attenuation (low Q). This is explained in Figure 8, which shows peak frequency dropping to zero as Q falls below some threshold value. This threshold gets lower for thinner layers. The interpretation is that when attenuation becomes excessive, the PFS method estimates Q to be zero, even if Q is substantially greater than zero.

For better analyzing the results of our simulations, we will look at the summary statistics of the results (5 techniques, 3 methods, 10 bandwidths, and 100 traces for each) as follows. The conventional standard deviation merely indicates the oscillation of values around mean values, regardless of the deviation from the real Q. Since the deviation of estimation Q from the real Q can tell us the concentration of the results around the

real Q, it becomes an indicator of efficacy of a particular method or technique. Thus, the relative standard deviation to real Q is calculated from the difference between the estimated Q and real Q values, instead of the sample mean.

$$S = \sqrt{\sum \left(Q_{real} - Q_{est}\right)^2} \Big/ N \qquad (8)$$

The relative standard deviations to real Q for all methods and techniques are shown in figure 9. Figure 9a shows the standard deviation from the calculation of each attenuation model, while in figure 9b the standard deviation is derived from the result of each effective-bandwidth coefficient. In figure 9a, we can see that those 15 combinations of methods and techniques perform better when the estimated attenuation model has a low Q, except for the PFS method when Q<60. This is caused by the decrease of the relative error of calculation. When the quality factor rises up, the frequency shift decreases with less attenuation. From the equation (1), (2) and (4), the frequency shift primarily determines the estimated quality factor. The less the shift, the higher the relative error. In figure 9b, the relatively low standard deviation was taken from only technique I when effective-bandwidth coefficient is equal to 0.1. The PFS method has stable standard deviations, since its peak frequency, which determines the estimated Q, has no connection with the target bandwidth.

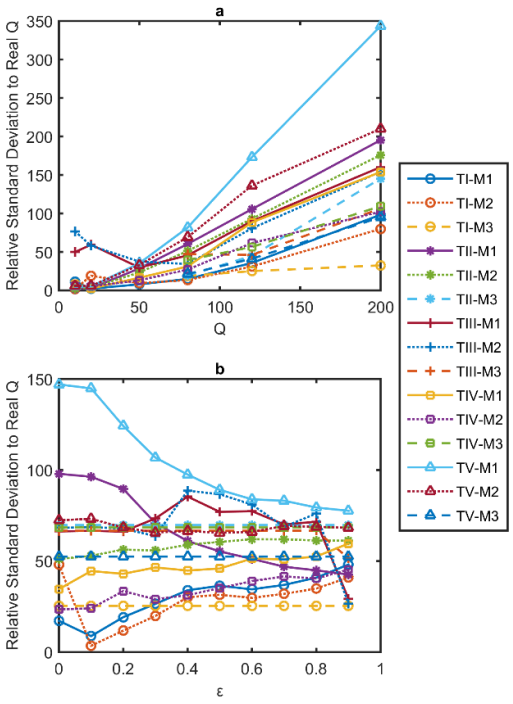

Fig. 9 **a**: The relative standard deviation to real Q with different attenuation models; **b**: the relative standard deviation to real Q with different bandwidths. TI-M1 represents the combination of technique I and method 1(CFS), TI-M2 represents the combination of technique I and method 2(SRM), TI-M3 represents the combination of technique I and method 3(PFS), etc.

Figure 10 compares the methods and techniques based on standard deviation. It proves that the technique I and IV are better than the other techniques and the technique I is the best among those techniques. Also, the SRM performs much better than CFS and PFS when applying technique IV as data pre-processing. This is in accord with the analysis in figure 9.

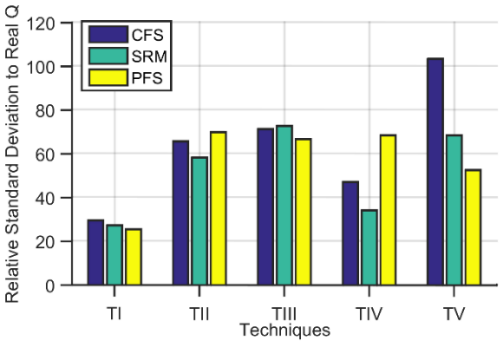

Fig.10 Relative standard deviation to real Q of each method and technique combinations for all effective-bandwidth coefficients and Q models

Conclusion

Three main Q estimating approaches have been specifically analyzed. Although the scattering or other frequency-independent factors do not contribute to the disturbance of Q estimation, accurate Q extraction from seismic reflection data, especially for pre-stack data is still difficult because of much more noise interference and more difficult interface tracking.

For the three frequency-domain methods, five kinds of pre-processing procedures were implemented. The PFS method has an inherent limitation to severe attenuation. Additionally, bandwidth choice is essential to all of those estimation methods because they are all primarily determined by the frequency shift. Generally, the effective-bandwidth coefficient of 0.1~0.3 is a good value. As for the data pre-processing techniques, it seems that the simplest one (TI) performs the best. But we could expect that some later techniques might perform better once in practice where there is much more noise and perhaps tuning effect because of the stronger capability of denoising. We plan to investigate the role of noise of tuning in future studies.

EDITED REFERENCES

Note: This reference list is a copyedited version of the reference list submitted by the author. Reference lists for the 2016 SEG Technical Program Expanded Abstracts have been copyedited so that references provided with the online metadata for each paper will achieve a high degree of linking to cited sources that appear on the Web.

REFERENCES

Aldridge, D. F., 1990, The Berlage wavelet: Geophysics, **55**, 1508–1511, http://dx.doi.org/10.1190/1.1442799.

Bath, M., 1974, Spectral analysis in geophysics: Development in Solid Earth Geophysics, **7**, 563.

Cheng, P., and G. F. Margrave, 2013, Estimation of Q: A comparison of different computational methods: CSPG/CSEG/CWLS GeoConvention, **12**, 2–5.

Dasgupta, R., and R. A. Clark, 1998, Estimation of Q from surface seismic reflection data: Geophysics, **63**, 2120–2128, http://dx.doi.org/10.1190/1.1444505.

Engelhard, L., 1996, Determination of seismic-wave attenuation by complex trace analysis: Geophysics Journal International, **125**, 608–622, http://dx.doi.org/10.1111/j.1365-246X.1996.tb00023.x.

Frisillo, A. L., and T. J. Stewart, 1980, Effect of partial gas/brine saturation on ultrasonic absorption in sandstone: Journal of Geophysical Researches, **85**, 5209–5211, http://dx.doi.org/10.1029/JB085iB10p05209.

Gladwin, M. T., and F. D. Stacey, 1974, Anelastic degradation of acoustic pulses in rock: Physics of the Earth and Planetary Interiors, **8**, 332–336, http://dx.doi.org/10.1016/0031-9201(76)90068-6.